New Series of Ni(II), Cu(II), Zr(IV), Ag(I), and Cd(II) Complexes of Trimethoprim and Diamine Ligands: Synthesis, Characterization, and Biological Studies

Amaal Younis Al-Assafe[1*] and Rana Abdul Malik Sulaiman Al-Quaba[2]

[1]*Department of Chemistry, College of Education for Pure Science, University of Mosul, Mosul 41001, Iraq*

[2]*Department of Chemistry, College of Science, University of Mosul, Mosul 41001, Iraq*

* ***Corresponding author:***

email: amaalyounis62@uomosul.edu.iq

Received: September 20, 2023
Accepted: January 11, 2024

DOI: 10.22146/ijc.89167

Abstract: *New compounds series of [M(TMP)(en)]X·nH$_2$O and [M(TMP)(PD)]X·nH$_2$O, where M = Ni^{2+}, Cu^{2+}, Zr^{4+}, Ag^{+}, Cd^{2+}, TMP = trimethoprim, en = ethylenediamine, PD = o-phenylene and X= Cl^{-} or NO$_3^{-}$, were prepared. The compounds were characterized using techniques including melting points, conductance, elemental analysis, FTIR, NMR, and mass spectroscopy. FTIR spectra indicated TMP acted like a bi-dentate ligand, combining via the nitrogen atoms of azomethine and pyrimidine amino groups. Diamine ligands (en or o-PD) are coordinated via two nitrogen atoms. Prepared compounds showed monomeric behavior and adopted a 6-coordinate octahedral geometry based on magnetic susceptibility and UV spectra. Conductivity measurements revealed Zr(IV) compounds were 1:2 conductive, while Ag^{+} and Cd^{2+} were 1:1 conductive; Ni^{2+} and Cu^{2+} compounds were non-conductive. Antibacterial tests on compounds and ligands against* Bacillus subtilis *and* Staphylococcus aureus *demonstrated broad-spectrum antibacterial activity. The mixed metal compounds revealed an observable tendency of antibacterial activity in the order Zr > Cd = Ag > Cu, making Zr(IV) compounds the most biologically active among them against* S. aureus *(Gram-positive) while the same compounds showed less antibacterial activity against* B. subtilis *(Gram-negative) than the free ligand.*

Keywords: *antibacterial activity; chelating agent; diamine ligand; mixed ligands; trimethoprim*

■ INTRODUCTION

Trimethoprim compound, 5-(3,4,5-trimethoxybenzyl)pyrimidine-2,4-diamine (TMP) with a formula of $C_{14}H_{18}N_4O_3$ is an antibiotic. The molecular weight of this compound is 290.3 g mol^{-1} [1]. It finds widespread application in treating infections within the urinary tract, respiratory system, and middle ear [2-3], owing to its strong binding to a bacterial enzyme that hinders the creation of tetrahydrofolic acid [4]. Due to its composition of N and O atoms, trimethoprim acts as a multi-dentate ligand, forming comprehensive compounds with metal ions [5]. In combination with other ligands like bipy and 1,10-phen, it forms mixed ligands that demonstrate stability in biological, organic, and thermal contexts [6]. Notably, there's potential for antitumor cytotoxicity [7]. However, mixed metal compounds of trimethoprim have received limited attention. Because they are essential to biological systems, they have been studied.

One method used in chemotherapy to induce pharmaceuticals activity is metal-ligand (drug) complexation. Chelation can increase the metabolic activity of bioactive species as well the metal ion polarity decreases by chelation through partially sharing the positive charge (metal ion) and overlapping the orbital ligand [8]. Furthermore, these compounds increase the cell respiration rate, which limits the organism's growth by disrupting the synthesis of proteins. Transition metal complexes are cationic, neutral, or anionic entities that are coordinated by ligands, where ligands are used to

coordinate with transition metal. Transition metal ions have been shown to serve essential roles in the human body's biological processes. Both Zn^{2+} and Cu^{2+} ions, for instance, are the second and third most common metal ions in humans. They present in many enzymes as structural elements or in the active areas. Vitamin B12 contains cobalt, a co-enzyme that is important for a number of metabolic processes. There are various transition metals that are potent therapeutic agents, particularly when coupled to a ligand to create metal compounds [9]. A compounds list contains metals that are utilized in chemotherapy to treat various illnesses including Pt (anticancer), Ag (antimicrobial), Au (antiarthritic), Bi (antiulcer), Sb (antiprotozoal), V (antidiabetic), and Fe (antimalaria) [10]. It was suggested that Ag functions by attaching itself to important functional regions of enzymes. The cytoplasmic membrane of bacteria, which is linked to numerous important enzymes, is a prime target for Ag^{+} because it induces the release of K^{+} ions from bacteria. Many antibacterial drugs block critical processes that lead to the synthesis of peptidoglycan, (building block bacteria's cell wall) compounds' stability prevents the Cd^{2+} in the test media from liberating, despite the fact that the cadmium salts are toxic. Additionally, human ligands and compounds are not dangerous to humans, but cadmium salts are [11].

There are few studies on trimethoprim mixed metal compounds [12]. This study aims to prepare, recognize, and assess the antibacterial properties of Ni(II), Cu(II), Zr(IV), Ag(I), and Cd(II) compounds. These compounds incorporate mixed trimethoprim ligands, specifically ethylenediamine and *o*-phenylenediamine. We choose these metal ions due to their broad biological activity.

■ EXPERIMENTAL SECTION

Materials

Since every compound employed was of analytical grade, no additional purification was necessary. Before being used, the reagents were not further purified. Trimethoprim was acquired from Samarra, Iraq's state enterprise for the pharmaceutical industries and medical appliances (SDI). Metal chlorides, [$NiCl_2{\cdot}6H_2O$], and [$CuCl_2{\cdot}2H_2O$], metal nitrates, [$ZrO(NO_3)_2{\cdot}H_2O$], $AgNO_3$, and [$Cd(NO_3)_2{\cdot}4H_2O$], ethylenediamine, *o*-phenylenediamine were supplied from Sigma Aldrich. Ethanol and dimethyl formamide (DMF) were provided by Fluka Company.

Instrumentation

Melting point determination for ligands and compounds was carried out using SMP30 equipment. Metal ion analyses were performed using the Analytic Jena GmbH-novAA350-Flame Atomic Absorption Spectrometer at the Agriculture College and Forestry, Mosul University. The molar conductance of the produced compounds was measured using a HANNA EC214 conductivity meter in DMF at 25 °C. Magnetic susceptibility measurements for generated compounds were conducted using the Sherwood Scientific MK1 instrument. Infrared absorption spectra were recorded utilizing a Shimadzu FTIR 84005 Spectrophotometer within the 400–4000 cm^{-1} range, employing potassium bromide and cesium iodide desks. For the determination of ^{1}H- and ^{13}C-NMR spectra of certain compounds, a Bruker DRX system operating at 400 MHz was utilized, with TMS in DMSO-d_6. The molecular weight of the ligand (L_1) and complex (5) was determined using the Shimadzu GC-MS-Q Ultra Gas Chromatography-Mass Spectrometry measurement device at the laboratory center of Samarra University. Electronic spectra measurements for ligands and their compounds at a concentration of 10^{-3} M in DMF at 25 °C were conducted using the Shimadzu UV-vis spectrophotometer Ultraviolet-1800 at 190–1100 nm.

Procedure

Synthesis of metal ions complexes

$$MCl_2{\cdot}nH_2O + tmp + en/phen \rightarrow \left[M(tmp)(en)Cl_2\right]{\cdot}nH_2O,\ \left[M(tmp)(phen)Cl_2\right]{\cdot}nH_2O$$

$M = Ni,\ Cu \quad n=0,2$

$$\left[ZrO(NO_3)_2{\cdot}H_2O\right] + tmp + en/phen \rightarrow \left[ZrO(tmp)(en)H_2O\right](NO_3)_2{\cdot}H_2O,\ \left[ZrO(tmp)(phen)H_2O\right](NO_3)_2{\cdot}H_2O$$

$$AgNO_3\left[Cd(NO_3)_2{\cdot}4H_2O\right] + tmp + en/phen \rightarrow \left[M(tmp)(en)\right]X{\cdot}H_2O,\ \left[M(tmp)(phen)\right]{\cdot}xNO_3{\cdot}H_2O$$

M = Ag, Cd X=1,2

An ethanolic solution containing 1 mmol of metal chlorides ([$NiCl_2·6H_2O$] (0.237 g), [$CuCl_2·2H_2O$] (0.170 g)) or metal nitrate ([$ZrO(NO_3)_2·H_2O$] (0.267 g), [$AgNO_3$] (0.170 g), [$Cd(NO_3)_2·4H_2O$] (0.308 g)) was carefully added in a stepwise manner to a solution of the ligand by dissolving 1 mmol of TMP (L_1) (0.290 g) and en (L_2) (0.060 g) or PD (L_3) (0.108 g) in 20 mL ethanol. The reaction mixture was refluxed for about 3–4 h. The resultant colored product was then cooled, filtered, and washed by ether.

Study of the bacterial activity of the prepared compounds

The Hinton Mueller agar culture medium was prepared following the guidelines provided by the Indian company. To make the medium, 38 g of agar was dissolved in 1 L of distilled water that had been previously boiled. The medium pH was adjusted to neutral, and then the solution was transferred to an autoclave. It was subjected to 121 °C and a pressure of 150 pounds/inch for 15 min. Then, the solution temperature was cooled down to 50 °C. Next, the culture solution was poured into Petri dishes, with a thickness of 2 mm per dish, and allowed to settle. Then the dishes were placed in an incubator at 37 °C for 24 h to prevent any potential contamination. This step was taken to ensure the purity of the culture.

In our research, 1 mL solution was formulated at a concentration of 10 µg dissolved in DMSO solvent. Subsequently, 100 µm of these solutions were introduced into perforations in the culture medium. The Petri dishes were then sealed using specialized tape and, placed within an incubator for 24 h at about 37 °C. For comparison, ciprofloxacin antibiotic was employed as a control.

■ RESULTS AND DISCUSSION

Table 1 includes the analytical data as well as the physical characteristics of the compounds. Each compound exhibits constant temperature stability and is insensitive to airborne moisture and oxygen. All organic solvents, with the exception of DMF and DMSO, proved insoluble for them. There is an acceptable degree of agreement between the elemental analysis conclusions and the results obtained.

Infrared Spectroscopy

Based on a comprehensive analysis of their spectra, we delved into the FTIR spectra of trimethoprim, diamine ligands (en or PD), and their corresponding metal compounds (Table 2). The pyrimidine amino group (NH_2) exhibits both asymmetric and symmetric stretching vibrations. Initially detected in TMP at wavenumbers 3467 and 3317 cm^{-1} [11], were found to persist in the complexes within the range of 3300–3412 cm^{-1}. This observation verified the amino nitrogen's attachment to metal(II) ions without deprotonation [12-13].

Table 1. Physical properties of TMP(L1) co-ligands (en, PD) and prepared compounds

No.	Compounds	Color	M.P	Yield	M.Wt	% CHN analysis calc (found)			% Metal
					g mol^{-1}	C	H	N	found (calc)
L_1	$C_{14}H_{18}N_4O_3$ (TMP)	White	238–240	--	290.32	57.93 (57.45)	6.20 (5.98)	19.28 (18.98)	---
L_2	$C_2H_8N_2$ (en)	Colorless	8	--	60.10	39.93 (39.76)	13.31 (12.65)	46.58 (46.18)	---
L_3	$C_6H_8N_2$ (PD)	Orange-brown	100–102	--	108.10	66.60 (65.11)	7.40 (7.00)	25.90 (25.35)	---
1	[Ni(tmp)(en)Cl_2]	Pink	206–208	95	480.01	39.99 (39.93)	5.35 (5.21)	17.49 (17.22)	12.22 (11.45)
2	[Cu(tmp)(en)Cl_2]·$2H_2O$	Dark brown	188–190	92	520.87	36.86 (36.37)	5.75 (5.24)	16.12 (15.73)	12.20 (11.69)
3	[ZrO(tmp)(en)H_2O]$(NO_3)_2$·H_2O	Yellow	190–192	98	617.55	31.09 (30.78)	4.85 (4.25)	18.13 (17.87)	14. 77 (14.36)
4	[Ag(tmp)(en)]NO_3·H_2O	Dark gray	145–147	96	538.29	35.66 (35.11)	5.20 (4.86)	18.20 (17.79)	20.03 (19.87)
5	[Cd(tmp)(en)]$(NO_3)_2$·H_2O	Yellowish white	130–132	91	604.83	31.74 (31.33)	4.62 (4.23)	16.20 (15.59)	18.58 (18.22)
6	[Ni(tmp)(PD)Cl_2]	Violet	214–216	93	527.91	45.46 (45.20)	3.78 (3.11)	15.91 (15.53)	11.11 (10.72)
7	[Cu(tmp)(PD)Cl_2]·$2H_2O$	Brown	198–200	92	568.77	42.19 (41.98)	5.27 (4.66)	14.76 (14.33)	11.17 (10.84)
8	[ZrO(tmp)(PD)H_2O]$(NO_3)_2$·H_2O	Reddish brown	200–202	81	655.54	36.06 (35.92)	4.50 (4.22)	16.82 (16.68)	13.70 (13.32)
9	[Ag(tmp)(PD)]NO_3·H_2O	Gray	153–155	90	586.19	40.94	4.77 (4.49)	16.71 (16.27)	18.40 (17.99)
10	[Cd(tmp)(PD)]$(NO_3)_2$·H_2O	Milky white	138–140	90	652.73	36.76 (36.33)	4.28 (3.8)	17.15 (16.78)	17.22 (16.82)

Table 2. FTIR bands of the mixed ligands (L_1, L_2, L_3) and their metal ion complexes in cm^{-1}

No.	Compounds	νNH₂ asym.	νNH₂ sym.	νNH₂ En\PD	νC=N Pyrimidine	νC=C	νM-N	νM-Cl	νM=O νM-O	νH₂O	Others
L_1	TMP	3467	3317	--	1633	1593	---	---	---	---	---
L_2	EN	---		3424, 3335	---	---	---	---	---	---	---
L_3	PD	---		3380, 3363	---	---	---	---	---	---	$P_tNH_2$1153, $P_WNH_2$1057, $P_rNH_2$925
1	[Ni(tmp)(en)Cl₂]	3469	3326	3294	1641	1593	516	381	--	--	$P_tNH_2$1126, $P_WNH_2$1022, $P_rNH_2$802
2	[Cu(tmp)(en)Cl₂]·2H₂O	3448	3318	3190	1665	1590	533	388	--	--	$P_tNH_2$1122, $P_WNH_2$1047, $P_rNH_2$830, νOH676
3	[ZrO(tmp)(en)](NO₃)₂·2H₂O	3465	3394	3280	1641	1589	594	--	993, 453	3515	$P_tNH_2$1128, $P_WNH_2$1053, $P_rNH_2$815, νOH682
4	[Ag(tmp)(en)]NO₃·H₂O	3467	3317	3280	1637	1575	588	--	--	3600	$P_tNH_2$1126, $P_WNH_2$1043, $P_rNH_2$821, νOH684
5	[Cd(tmp)(en)](NO₃)₂·H₂O	3410	3320	3195	1666	1590	525	--	--	3465	$P_tNH_2$1128, $P_WNH_2$1062, $P_rNH_2$833, νOH 678
6	[Ni(tmp)(PD)Cl₂]	3398	3321	3190	1639	1593	516	--	--	3550	$P_tNH_2$1127, $P_WNH_2$1021, $P_rNH_2$825
7	[Cu(tmp)(PD)Cl₂]·2H₂O	3450	3332	3186	1670	1591	555	391	--	3569	$P_tNH_2$1120, $P_WNH_2$1045, $P_rNH_2$829, νOH671
8	[ZrO(tmp)(PD)](NO₃)₂·H₂O	3434	3328	3234	1647	1560	532	--	1000, 464	3519	$P_tNH_2$1124, $P_WNH_2$1054, $P_rNH_2$829, νOH678
9	[Ag(tmp)(PD)]NO₃·H₂O	3465	3319	3281	1640	1578	593	--	--	3590	$P_tNH_2$1128, $P_WNH_2$1045, $P_rNH_2$819, νOH683
10	[Cd(tmp)(PD)](NO₃)₂·H₂O	3398	3321	3190	1664	1593	516	--	--	3550	$P_tNH_2$1128, $P_WNH_2$1062, $P_rNH_2$833, νOH 678

Asym. = asymmetric, sym. = symmetric

A discernible reduction in the ν(C=N) value was noted within the range of 6–33 cm^{-1}, indicative of a shift in the peak of this group. This shift signified the coordination site originating from the atom of the nitrogen of azomethine group [14-15]. Additional bands emerged in all of the spectra, and they were assigned to the M–NTMP bond, thus showing the nitrogen atoms interacting in coordination with the metal ions [16].

A distinctive band related to the ethylene di amine's (N–H) stretching was observed at a slightly lower frequency range of 3211–3270 cm^{-1}. This provided evidence of its interaction with the metal ions. The ν(M–N) stretching frequencies emerged at 510–626 cm^{-1}. Similarly, the stretching vibrations of the NH_2 groups, seen at 3383–3364 cm^{-1} in the PD spectrum, exhibited a shift to lower frequencies in the complex spectra at 3210–3379 cm^{-1}. This shift indicated the involvement of NH_2 groups in coordination. Further evidence of this coordination was seen in the bending peaks of the NH_2 groups, which moved to lower frequencies, specifically at 1150–1134 cm^{-1} for tNH_2, 1115–1072 cm^{-1} for wNH_2, and 826–822 cm^{-1} for rNH_2 [17].

Additionally, new bands emerged at wavenumbers 949–1032 and 418–467 cm^{-1}, and these were attributed to νM=O bonds [18]. The band appeared in the domain of 3414–3420 cm^{-1}, accompanied by two weaker bands that could be identified as O–H stretching. These features pointed to the fact that coordination water molecules were present in the Zr(IV) compound structure [19]. Moreover, the bands that appeared at 370–381 cm^{-1} were ascribed to stretching vibrations of ν(M–Cl) [20] as seen in Fig. S1-S3.

Magnetic, Spectral Studies and Conductivity Measurements

The relevant UV-vis data is in Table 3. The UV spectrum of trimethoprim exhibited two distinct peaks

(Fig. S4). The first peak arose from an intra-ligand transition within the aromatic (C=C) group, specifically the π→π* transition, occurring at a wavenumber of 40,088 cm^{-1}. The second peak, positioned at 34,423 cm^{-1}, resulted from the n→π* transition induced by the nitrogen atom in the imine (-C=N-) group (Table 3) [21]. The compounds displayed absorption peaks within the ranges of 33557–35587 and 31446–33333 cm^{-1}, related to the π→π* and n→π* transitions respectively, taking place in aromatic ring and diamine compounds. These transitions observed a shift in metal compounds, clearly indicating coordination between the ligand and metal ion [22]. Regarding *d-d* transitions, the electronic spectrum of $[Ni(TMP)(en)Cl_2]$ revealed peaks at 12594 and 14368 cm^{-1}, due to the transitions $^3A_2g \rightarrow {}^3T_2g$ and $^3A_2g \rightarrow {}^3T_1g_{(F)}$, respectively. In general, octahedral and tetrahedral compounds of Ni(II) exhibited magnetic moments between 2.90–3.40 and 3.50–4.10 B.M, respectively, signifying their paramagnetic nature [23]. Square planar of Ni(II) compounds, on the other hand, were diamagnetic. The magnetic susceptibility value of 2.2 B.M for the nickel(II) compound indicates that the high and low spin octahedral forms are in equilibrium [24].

Moving on to the copper complex $[Cu(TMP)(en/PD)Cl_2]\cdot 2H_2O$, it displayed distorted octahedral geometry and manifested unsymmetrical absorption at 13,369 and 23,810 cm^{-1}. These absorptions were attributed to the $^2B_1g \rightarrow {}^2B_2g$ and $^2B_1g \rightarrow {}^2E_1g$ transitions of a tetragonal octahedral geometry, magnetic susceptibility value (1.8 BM) for Cu(II) complex confirmed its monomeric nature [25].

In the Zr(IV) compounds, intense peaks at 35714 and 37878 cm^{-1} indicated charge-transfer transitions [26]. The absence of visible region bands ruled out the presence of *d-d* electronic spectra. Peaks at 37,972 and 39,467 cm^{-1} were attributed to transfer charge from the donor ligand atoms to the Ag^+ ion, suggesting tetrahedral geometry [27]. The Cd^{2+} complex solely exhibited the metal to the ligand charge transfer transition, as expected, given the absence of *d-d* transitions. This complex was predictably tetrahedral and diamagnetic [28] (Fig. S5 and S6). Molar conductivities were measured in DMF at room temperature for compounds with a concentration of 10^{-3} M. The findings presented herein validate the compounds' non-conductance nature, and it is established that the chloride ion coordinates with Ni(II) and Cu(II) ions. The relatively low molar conductivities of the compounds, ranging from 27 to 30 Ω^{-1} cm^2 mol^{-1}, indicate their lack of electrolytic behavior when dissolved [29]. Conversely, the molar conductivity readings for Ag(I) compounds confirm their identity as 1:1 electrolytes, while those for Zr(IV) and Cd(II) compounds are indicative of ionic 1:2 behavior [28], as illustrated in Table 3.

Table 3. Electronic spectral data on metal complexes including ligands, molar conductivity, and magnetic moments

No.	Compound	Absorption (cm^{-1})	Assignment	μ_{eff} (B.M)	Λ_M (Ω^{-1} cm^2 mol^{-1})	Suggested structure
L_1	TMP	34423, 40088	n→π*, π→π*	--	--	--
L_2	EN	33557	n→π*	--	--	--
L_3	PD	31318, 35280	n→π*, π→π*	--	--	--
1	$[Ni(TMP)(en)Cl_2]$	34246, 14386, 12548	C.T, $^3A_2g \rightarrow {}^3T_1g$, $^3A_2g \rightarrow {}^3T_2g$	2.3	30	Octahedral
2	$[Cu()(en)Cl_2]\cdot 2H_2O$	35211, 23809, 13296	C.T, $^2B_1g \rightarrow E_1g$, $^2B_1g \rightarrow {}^2B_2g$	1.8	28	Octahedral
3	$[ZrO(TMP)(en)H_2O](NO_3)_2\cdot H_2O$	37313	C.T	0.0	140	Octahedral
4	$[Ag(TMP)(en)]NO_3\cdot H_2O$	34246	C.T	0.0	75	Tetrahedral
5	$[Cd(TMP)(en)](NO_3)_2\cdot H_2O$	36363	C.T	0.0	150	Tetrahedral
6	$[Ni(TMP)(PD)Cl_2]$	36490, 14368, 11335	C.T, $^3A_2g \rightarrow {}^3T_1g$, $^3A_2g \rightarrow {}^3T_2g$	2.5	27	Octahedral
7	$[Cu(TMP)(PD)Cl_2]\cdot 2H_2O$	37313, 23810, 13379	C.T, $^2B_1g \rightarrow E_1g$, $^2B_1g \rightarrow {}^2B_2g$	1.8	27	Octahedral
8	$[ZrO(TMP)(PD)H_2O](NO_3)_2\cdot H_2O$	35211	C.T	0.0	130	Octahedral
9	$[Ag(TMP)(PD)]NO_3\cdot H_2O$	37972, 39467	C.T	0.0	69	Tetrahedral
10	$[Cd(TMP)(PD)](NO_3)_2\cdot H_2O$	36366, 39572	C.T	0.0	155	Tetrahedral

NMR Spectra

The NMR ligand spectrum of L_1 and compounds 3 and 10 were obtained in DMSO-d_6 and are displayed in Table 4 (Fig. S7-S11). The ^{1}H-NMR spectrum of L_1 displays the protons signals of the NH_2 groups at 6.20 and 5.83 ppm. The singlet signal for the pyrimidine ring proton (–CH–N) is observed at 7.53 ppm. The aromatic protons are represented as multiples at 6.56 ppm. The OCH_3 protons appear as signals at 3.62 and 3.72 ppm, respectively. A signal for the CH_2 protons is observed at δ 3.54 ppm, and at 2.50 ppm, the DMSO signal is evident. In the ^{13}C-NMR spectra, chemical shifts of L_1 at 162.2 ppm are attributed to C=N, while shifts at 155.7 and 152.7 ppm correspond to carbon atoms in the C=C bonds of the pyrimidine ring. The aromatic carbon signals are observed at 105.8 and 135.0 ppm. Two additional chemical shifts are noted for C atoms at 55.8 and 33.0 ppm, respectively. The chemical shift due to DMSO-d_6 is observed at 40.2 ppm. The ligand L_1 and compounds 3 and 10 exhibit recorded ^{1}H- and ^{13}C-NMR spectra, as detailed in Table 4. Compounds 3 and 10 display signals corresponding to ligands L_2 and L_3 (en and PD), along with signals from ligand L_1. This consistency supports the proposed formulas for the compounds.

Mass Spectrum

Compounds 1, 10, and their molecular weight and fragmentation structure were determined using mass spectrometry (Fig. S12-S13). The suggested structure formula is located as follows, based on the findings mentioned in Fig. 1.

Bacterial Efficacy Application

The bacterial activity of prepared ligands and some of their metallic compounds was studied. This study encompassed the assessment of biological activity against specific types of bacteria identified in the laboratory through chemical and microscopic analyses. These isolated bacteria are responsible for numerous human diseases. The first type, Gram-negative bacteria, was represented by *B. subtilis* (ATCC 6633), while the second type, Gram-positive bacteria, was exemplified by *S. aureus* (ATCC 25923). The antibacterial activity analysis of all compounds is seen in Fig. S12 and S13. The inhibitory results, as shown in Table 5, indicate that some of the prepared compounds demonstrated the ability to inhibit the growth of the tested bacteria, and results revealed that the Zr(IV) metal compounds showed excellent antibacterial activity having a zone of inhibition against *S. aureus*. It is evident from these results that some metal ions like Zr(IV), on complexation, contribute to the ligand's sensitivity to microbial organisms. These results are compared with previous researches [30-31]. The ion metal's oxidation state, the

Table 5. The biological properties of tested compounds

S. aureus	*B. subtilis*	Prepared compounds
24	15	Control
16	14	L_1
14	12	Cu
16	7	Ag
16	6	Cd
20	11	Zr

Table 4. ^{1}H- and ^{13}C-NMR spectral data of TMP and some complexes

Compounds	^{1}H-NMR spectra	^{13}C-NMR spectra
L_1(TMP)	7.53 (1H, s), 6.56 (2H, s), 6.20 (2H, s), 5.83 (2H, s), 3.72 (6H, s), 3.62 (3H, s), 3.54 (2H, s)	162.2, 155.7, 152.7, 135.9, 135.7, 105.8, 6.0, 55.8, 33.0
$[ZrO(TMP)(en)H_2O](NO_3)_2{\cdot}H_2O$	7.51 (1H, s), 6.55 (2H, s), 6.16 (2H, s), 5.79 (2H, s), 4.65 (2H, s), 3.72 (6H, s), 3.61 (3H, s), 3.52 (2H, s), 3.17–3.08 (2H, m), 2.87–2.73 (4H, m)	162.3, 162.0, 155.2, 152.7, 135.9, 135.7, 105.9, 105.8, 60.0, 55.8, 33.0
$[Cd(TMP)(PD)](NO_3)_2{\cdot}H_2O$	7.30 (1H, s), 6.49 (1H, s), 6.42 (1H, dt, *J* = 7.3, 3.6 Hz), 6.30 (1H, dd, *J* = 5.7, 3.5 Hz), 5.90 (1H, s), 4.34 (1H, s), 3.66 (2H, s), 3.55 (1H, s), 3.46 (1H, s), 0.99 (1H, t, *J* = 7.0 Hz).	162.5, 152.8, 134.9, 117.3, 114.6, 106.0, 60.0, 55.9, 32.9, 18.6

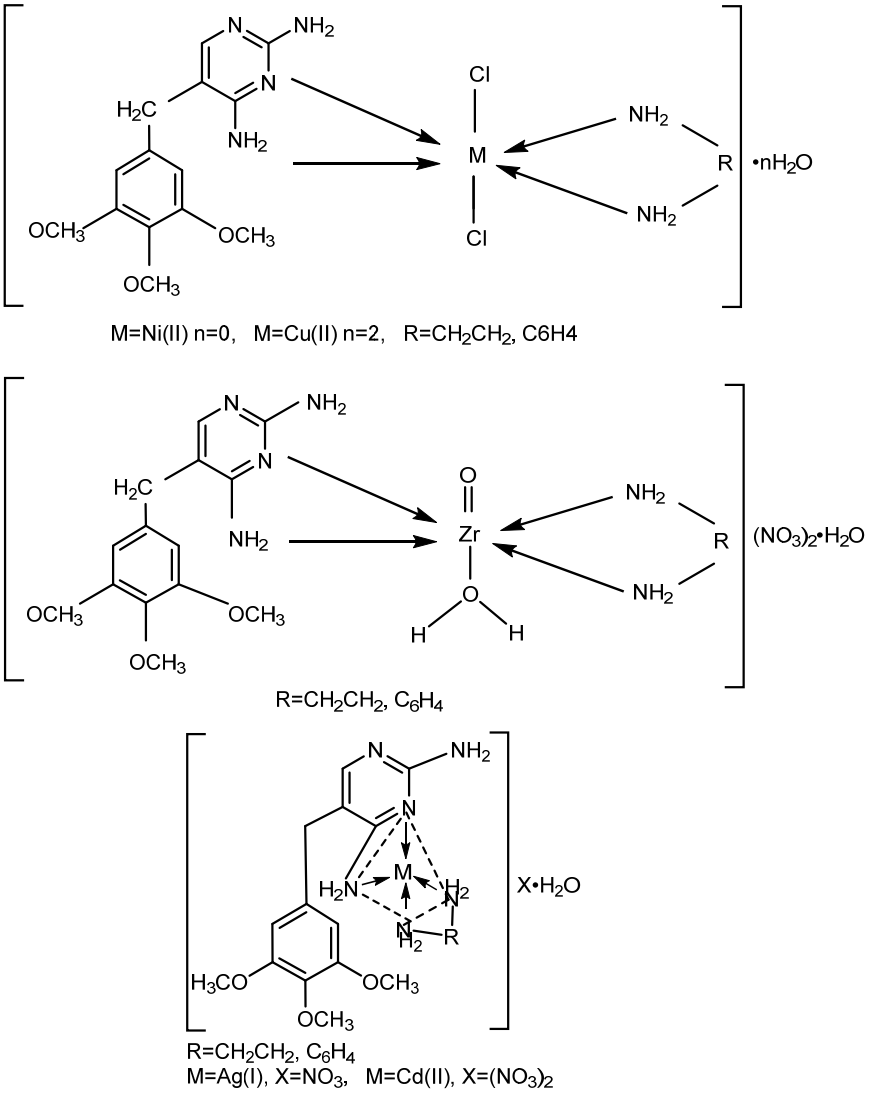

Fig 1. Suggested structure of the prepared complexes

overtone principle, and chelation theory can all be used to explain the increased activity of the metal chelates. The cell permeability overtone idea states that only lipid-soluble substances can pass through the lipid membrane around the cell, and that liposolubility plays a significant role in regulating the antimicrobial action. The metal ions polarity is greatly diminished by chelation. Elevated lipophilicity makes substances more soluble in membranes of lipid and prevents all metal binding locations in microorganism enzymes due to its *p*-electron delocalization on the entire chelating ring and partial sharing of positive charge with donor groups [15,32-35]. Compared to Gram-negative bacteria, Gram-positive bacteria are distinguished by a thicker layer of peptidoglycan and an outer membrane of lipids when none is present. This difference in bacterial membrane structure and cell wall composition, as well as the characteristics of ligands, metals, chelates, total charge of compounds, and nuclearity of metals in a complex, have all been linked to the effectiveness of metal compounds against Gram-positive bacteria [36-37]. This is evident in the prepared compounds, as they showed less activity against Gram-negative bacteria (*B. subtilis*) than the ligand.

■ CONCLUSION

Mixed-ligand compounds containing Ni^{2+}, Cu^{2+}, Zr^{4+}, Ag^{+}, and Cd^{2+} ions were synthesized and subjected to spectroscopic analysis. Infrared spectra revealed the

coordination of diamine ligands through the atoms of nitrogen of the diamine molecules. Meanwhile, TMP acted as a bidentate ligand, binding through the nitrogen atoms of the azomethine and pyrimidine groups. Electronic spectra data indicated that all compounds adopted monomeric octahedral and tetrahedral geometries. Interestingly, the compounds and their respective ligands displayed broad-spectrum antimicrobial activity against various bacterial strains.

■ ACKNOWLEDGMENTS

We are grateful to the Chemistry Department of the University of Mosul, Iraq's College of Science for giving us supplies for the research, including chemicals.

■ SUPPORTING INFORMATION

Fig. S1. FTIR spectrum of TMP ligand, Fig. S2. FTIR spectrum of $[ZrO(tmp)(PD)](NO_3)_2{\cdot}H_2O$, Fig. S3 FTIR spectrum of $[Ni(tmp)(en)Cl_2]$, Fig. S4. UV-vis spectrum of TMP ligand, Fig. S5. UV-vis spectrum of $[ZrO(tmp)(en)H_2O](NO_3)_2{\cdot}H_2O$, Fig. S6. UV-vis spectrum of $[Ag(tmp)(en)]NO_3{\cdot}H_2O$, Fig. S7. ^{1}H-NMR spectrum of TMP ligand, Fig. S8. ^{1}H-NMR spectrum of $[Cd(tmp)(PD)](NO_3)_2{\cdot}H_2O$, Fig. S9. ^{1}H-NMR spectrum of $[ZrO(tmp)(en)(H_2O)](NO_3)_2{\cdot}H_2O$, Fig. S10. ^{13}C-NMR spectrum of TMP ligand, Fig. S11. ^{13}C-NMR spectrum of $[Cd(tmp)(PD)](NO_3)_2{\cdot}H_2O$, Fig. S12. GC-MS data of $[Ni(tmp)(en)Cl_2]$, Fig. S13. GC-MS data of $[Cd(tmp)(PD)](NO_3)_2{\cdot}H_2O$, Fig. S14. Effect of different concentration of materials on the growth of (a) *B. subtillis* and (b) *S. aureus*, Fig. S15. Inhibition zones of complexes with ligands for two types of bacteria.

■ CONFLICT OF INTEREST

There are no conflicts of interest.

■ AUTHOR CONTRIBUTIONS

The researchers conducted the experiment, wrote and revised the manuscript. All authors approved the final version of this manuscript.

■ REFERENCES

[1] Eugene-Osoikhia, T.T., Ojeyemi, S.A., Akong, R.A., Oyetunde, T., Onche, E.U., and Ayeni, F., 2021, Synthesis, characterisation and antimicrobial studies of metal(II) complexes of trimethoprim and 2,2'-bipyridin heterocycle, *Niger. Res. J. Chem. Sci.*, 9 (1), 273–295.

[2] Ikpeazu, O.V., Otuokere, I.E., and Igwe, K.K., 2020, Determination of stability constant of trimethoprim-Zn(II) complex at different temperatures by continuous variation method, *Int. J. Novel Res. Phys. Chem. Math.*, 7 (2), 1–7.

[3] Akinyele, O.F., Adejayan, S.B., Durosinmi, L.M., Ayeni, A.O., and Ajayeoba, T.A., 2020, Interactions of metal ions with trimethoprim and metformin, *Int. J. ChemTech Res.*, 13 (2), 38–46.

[4] Lawal, A., Ayanwale, P.A., Obaleye, J.A., Rajee, A.O., Babamale, H.F., and Lawal, M., 2017, Synthesis, characterization and biological studies of mixed ligands nicotinamide-trimethoprim complexes, *Int. J. Chem. Mater. Environ. Res.*, 4 (1), 97–101.

[5] Ahmed, F.J., AbdAlqader, B.S., Haddad, R.A., Abed, R.R., and Saleh, M.Y., 2022, Preparation and diagnosis of Zn(II), Cd(II) and Hg(II) complexes with Schiff base ligand derived from trimethoprim, *Egypt. J. Chem.*, 65 (10), 359–366.

[6] Hassan, Z.M., Alattar, R.A., Abass, S.K., Mihsen, H.H., Abbas, Z.F., and Hussain, K.A., 2022, Synthesis, characterization and biological activity of mixed ligand (imine of benzidine and 1,10-phenanthroline) complexes with Fe(II), Co(II), Ni(II) and Cu(II), *Chem. Chem. Technol.*, 16 (1), 15–24.

[7] Kim, H.Y., Kang, H.G., Kim, H.M., and Jeong, H.J., 2023, Antitumor activity of trimethoprim-sulfamethoxazole against melanoma skin cancer through triggering allergic reaction and promoting immunity, *Int. Immunopharmacol.*, 123, 110742.

[8] Olagboye, S.A., and Adebawore, A.A., 2021, Synthesis, characterization, and antimicrobial studies of mixed ligand complexes of acetanilide and ampicillin with cobalt(II) and nickel(II) ions, *Global Sci. J.*, 9 (11), 1327–1338.

[9] Bhowmick, A.C., Dev Nath, B., and Moim, M.I., 2019, Coordination complexes of transition metals and Schiff base with potent medicinal activity, *Am. J. Chem.*, 9 (4), 109–114.

[10] Olagboye, S.A., 2022, Synthesis, characterization and antimicrobial activities of mixed ligand metals complexes with trimethoprim and potassium thiocyanate, *Eur. J. Appl. Sci.*, 10 (1), 428–439.

[11] Albahadly, H.H., Al-Haidery, N.H., and Al-Salami., B.K., 2021, Synthesis, biological activity trimethoprim derivative and the complexes, *J. Phys.: Conf. Ser.*, 2063 (1), 012014.

[12] Albedair, L.A., 2020, Iron(III), gold(III), platinum(IV) and palladium(II) trimethoprim drugs complexes: Synthesis, spectroscopy, morphology and anticancer assessments, *Rev. Roum. Chim.*, 65 (12), 1145–1152.

[13] Gülcan, M., Sönmez, M., and Berber, İ., 2012, Synthesis, characterization, and antimicrobial activity of a new pyrimidine Schiff base and its Cu(II), Ni(II), Co(II), Pt(II), and Pd(II) complexes, *Turk. J. Chem.*, 36, 189.

[14] Ahmed, E.M., Marzouk, N.A., Hessien, S.A., and Ali, A.M., 2011, Synthesis, reactions and antimicrobial activity of some new thienopyridine and thienopyrimidine derivatives, *World J. Chem.*, 6 (1), 25–31.

[15] Mohan, C., Kumar, V., Kumari, N., Kumari, S., Yadav, J., Gandass, T., and Yadav, S., 2020, Synthesis, characterization and antibacterial activity of semicarbazide based Schiff bases and their Pb(II), Zr(IV) and U(VI) complexes, *Adv. J. Chem., Sect. B*, 2 (4), 187–196.

[16] Al-Mukhtar, S.E., and Aghwan, M.T., 2013, Synthesis and characterization of 3-methoxypropyldithiocarbamate complexes with iron(II), cobalt(II), nickel(II), copper(II) and zinc(II) and their adducts with nitrogen base ligands, *Rafidain J. Sci.*, 24 (7), 50–59.

[17] Alajrawy Othman, I., Ibraheem Kaiss, R., and Hadi Huda, A., 2019, Vanadyl VO(II) with *o*-phenylenediamine complexes preparation and spectral characterization, *Res. J. Chem. Environ.*, 23, 43–49.

[18] Khanmetov, A.A., Hajiyeva, K.S., Khamiyev, M.J., Alieva, R.V., Azizbeyli, H.R., and Ahmedbekova, S.F., 2018, Synthesis of zirconyl naphthenates on the basis of oil acids and their applying as complex catalytical systems in the process of oligomerization (polymerization) of ethylene, *Azerb. Chem. J.*, 3, 91–98.

[19] Eugene-Osoikhia, T.T., Akinpelu, I.O., and Odiaka, T.I., 2019, Synthesis, characterization and antimicrobial studies of transition metal complexes of Schiff base derived from salicylaldehyde and L-tyrosine amino acid, *Niger. J. Chem. Res.*, 24 (1), 46–56.

[20] Hammoda, R.G., and Shaalan, N., 2023, Synthesis of Zn(II) and Co(II) complexes with a Schiff base derived from malonic acid dihydrazide for photo-stabilizers of polystyrene, *Indones. J. Chem.*, 23 (5), 1324–1340.

[21] Osowole, A.A., Wakil, S.M., and Alao, O.K., 2015, Synthesis, characterization and antimicrobial activity of some mixed trimethoprim-sulfamethoxazole metal drug complexes, *World Appl. Sci. J.*, 33 (2), 336–342.

[22] Ishola, K.T., Olaoye, O.J., Oladipo, M.A., Odedokun, O.A., and Aboyeji, O.O., 2023, Synthesis, characterization and antimicrobial properties of mixed-ligand complexes of some metal(II) ions with barbituric acid and 1,10-phenanthroline ligands, *Tanz. J. Sci.*, 49 (2), 491–502.

[23] Al Alsultan, F.S., and Al Quaba, R.A.S., 2021, Preparation, spectral characterization, DFT and antibacterial study of new azo ligand derived from 2-aminoanthracene-9,10-dione with antipyrine mixed ligand complexes involving 1,10-phenanthroline ligand, *Egypt. J. Chem.*, 64 (11), 6635.

[24] Chen, Z., Lhoussain, K., Bucher, C., Jacquemin, D., Luneau, D., and Siri, O., 2020, Unconventional access to a solvatochromic nickel(II) dye featuring a coordination-induced spin crossover behavior, *Dyes Pigm.*, 183, 108645.

[25] Numan, A.T., Atiyah, E.M., Al-Shemary, R.K., and Abd_Ulrazzaq, S.S., 2018, Composition, characterization and antibacterial activity of Mn(II), Co(II), Ni(II), Cu(II) Zn(II) and Cd(II) mixed ligand complexes Schiff base derived from trimethoprim with 8-hydroxy quinoline, *J. Phys.: Conf. Ser.*, 1003 (10, 012016.

[26] Bhavani, S.D., Reddy, N.N., Raju, A.K., Radhika, M., Reddy, P.M., and Bhaskar, K., 2021, Synthesis and characterization of oxo zirconium(IV) complexes of polydentate ligands, *AIP Conf. Proc.*, 2369 (1), 020044**.**

[27] Bormio Nunes, J.H., de Paiva, R.E.F., Cuin, A., Lustri, W.R., and Corbi, P.P., 2015, Silver complexes with sulfathiazole and sulfamethoxazole: Synthesis, spectroscopic characterization, crystal structure and antibacterial assays, *Polyhedron*, 85, 437–444.

[28] Hassan, M.M.A., Abbas, A.H., Abed, E.H., and Abodi, E.E., 2018, Synthesis, characterization and antimicrobial activity of V(IV), Ag(I) and Cd(II) complexes with mixed ligands derived from sulfamethoxazole and trimethoprim, *Adv. Anal. Chem.*, 8 (2), 15–21.

[29] Alaghaz, A.N.M.A., Farag, R.S., Elnawawy, M.A., and Ekawy, A.D.A., 2016, Synthesis and spectral characterization studies of new trimethoprim-diphenyl phosphate metal complexes, *Int. J. Sci. Res.*, 5 (1), 1220–1229.

[30] Sadeek, S.A., Abd El-Hamid, S.M., and Zordok, W.A., 2018, Spectroscopic, DFT and antimicrobial activity of Zn(II), Zr(IV), Ce(IV) and U(VI) complexes of *N,N*- chelated 4,6-bis(4-chlorophenyl)-2-amino-1,2-dihydropyridine-3-carbinitrile, *Appl. Organomet. Chem.*, 32 (9), e4457.

[31] Al-Alzawi, S.M., Al-Jibouri, M.N., Rasheed, A.M., and Al-Bayati, S.M., 2023, Synthesis, characterization and antimicrobial activity of complexes metal ions Ni(II), Zn(II), Pd(II) and Pt(IV) with polydentate 1,2,4-triazole ligand, *Indones. J. Chem.*, 23 (1), 210–218.

[32] Mahind, L.H., Waghmode, S.A., Nawale, A., Mane, V.B., and Dagade, S.P., 2015, Evaluation of antimicrobial activities of zirconium(IV) complex, *IOSR J. Pharm. Biol. Sci.*, 5 (4), 102–105.

[33] Prakash, B.S., Raj, C.I.S., and Raj, G.A.G., 2017, Zr(IV) and Th(IV) Complexes with Schiff base ligands: Synthesis, characterization, antimicrobial studies, *Int. Refereed J. Eng. Sci.*, 6 (10), 43–53.

[34] Abdalrazaq, E., Jbarah, A.A.Q., Al-Noor, T.H., Shinain, G.T., and Jawad, M.M., 2022, Synthesis, DFT calculations, DNA interaction, and antimicrobial studies of some mixed ligand complexes of oxalic acid and Schiff base trimethoprim with various metal ions, *Indones. J. Chem.*, 22 (5), 1348–1364.

[35] Vitomirov, T., Čobeljić, B., Pevec, A., Radanović, D., Novaković, I., Savić, M., Anđelković, K., and Ristović, M.Š., 2023, Binuclear azide-bridged hydrazone Cu(II) complex: Synthesis, characterization and evaluation of biological activity, *J. Serb. Chem. Soc.*, 88 (9), 877–888.

[36] Kargar, H., Ardakani, A.A., Tahir, M.N., Ashfaq, M., and Munawar, K.S., 2021, Synthesis, spectral characterization, crystal structure and antibacterial activity of nickel(II), copper(II) and zinc(II) complexes containing ONNO donor Schiff base ligands, *J. Mol. Struct.*, 1233, 130112.

[37] Es-Sounni, B., Nakkabi, A., Bouymajane, A., Elaaraj, I., Bakhouch, M., Filali, F.R., El Yazidi, M., El Moualij, N., and Fahim, M., 2023, Synthesis, characterization, antioxidant and antibacterial activities of six metal complexes based tetradentate salen type bis-Schiff base, *Biointerface Res. Appl. Chem.*, 13 (4), 333.